Red Sea
Ocean rift
Hydrothermal activity
Sea floor spreading
Recent tectonics

Mer Rouge
Rift océanique
Hydrothermalisme
Expansion océanique
Tectonique récente

Geology of the Red Sea transitional region (22°N-25°N)

Enrico Bonatti [a], Paolo Colantoni [b], Bruno Della Vedova [c], Marco Taviani [b]
[a] Lamont-Doherty Geological Observatory, Columbia University, Palisades, New York 10964, U.S.A.
[b] Istituto di Geologia Marina del CNR, via Zamboni 65, Bologna, Italy
[c] Istituto di Miniere e Geofisica Applicata, Universita di Trieste, via Gessi 4, Trieste, Italy.

Received 26/4/83, in revised form 15/3/84, accepted 16/4/84.

ABSTRACT

The Red Sea between 22°N and 25°N is transitional between the southern Red Sea, where an axial rift valley with strong magnetic signature is almost continuous, and the Northern Red Sea where the axial valley and associated magnetic anomalies are absent. Segments of sediment-free axial trough with associated magnetic anomalies alternate with intertrough zones. The axial troughs and deeps are not aligned but show lateral offsets. The Nereus trough has an axial rift valley morphology and is carpeted by basalts with MORB affinity, indicating emplacement of oceanic type crust; magnetic anomalies suggest sea floor spreading initiated about 2-3 m.y.b.p. at the Nereus segment, but only 1 m.y.b.p. at the segment's northern tip, the implications being that Nereus is a mini-propagating oceanic rift. Heat flow within the Nereus trough ranges from very high (>2.000 mW/m^2) to very low (<100 mW/m^2), indicating sub-sea floor hydrothermal convective circulation, confirmed by the presence of brine pools and of metalliferous deposits. A basaltic seamount protruding through the sediments at the axis of the Bannock Deep, a subdued axial graben to the north of Nereus, may indicate punctiform initiation of another oceanic segment. Vine-Matthews magnetic anomalies were not detected in other axial deeps to the north of the Nereus trough or in inter-trough zones. Magnetic anomalies outside the axis are very subdued and heat flow is rather constant ($\simeq 150$ mW/m^2). A prominent reflector, probably the top of Miocene evaporites found elsewhere in the Red Sea, is almost ubiquitous in this region. Pre-and/or syn-evaporite tectonics can be detected in the reflection profiles. Observations from Zabargad island, an uplifted block of lithosphere 50 km West of the Red Sea axis, suggest that attenuated continental crust injected by basaltic dykes is present in this region outside the axial trough segments. The orientation of the Red Sea axis changes by about 50° at the Transitional Region, which is crossed by a fracture zone (Zabargad Fracture Zone) parallel to the Dead Sea fault and probably inherited from a pre-Red Sea lineament. The complex tectonics of this region can be related to its location near the front of a northward-propagating oceanic rift, which impinges against the Zabargad Fracture Zone, with formation of areas of extension and of compression related to the uplift of Zabargad Island.

Oceanol. Acta, 1984, 7, 4, 385-398.

RÉSUMÉ

Géologie de la Mer Rouge dans la région de transition entre 22°N et 25°N

La région de la Mer Rouge comprise entre 22°N et 25°N fait transition entre la partie méridionale, où la vallée axiale au magnétisme marqué est presque continue, et la partie septentrionale, sans vallée axiale ni anomalies magnétiques. Des tronçons de la fosse axiale dépourvus de sédiment et avec des anomalies magnétiques, alternent avec des zones interfosses. Les fosses axiales et les dépressions ne sont pas alignées, mais présentent des décalages latéraux. La fosse Nereus a une morphologie de vallée axiale tapissée de basaltes avec affinité MORB, indiquant l'emplacement d'une croûte de

type océanique; les anomalies magnétiques suggèrent que l'expansion océanique a débuté vers 2 ou 3 millions d'années B.P. sur le segment Nereus, mais seulement 1 million d'années B.P. sur sa pente nord, suggérant que Nereus est un rift océanique de faible intensité. Le flux de chaleur couvre une gamme allant de valeurs très fortes (> 2000 mW.m^{-2}) à très basses (< 100 mW.m^{-2}), traduisant une circulation convective hydrothermale peu profonde, confirmée par la présence de bassins de saumures et de dépôts métallifères. Un relief basaltique dominant les sédiments dans l'axe de la fosse Bannock et un fossé axial peu marqué au nord de Nereus, peuvent indiquer le point de départ d'un autre segment océanique. Les anomalies magnétiques de Vine-Matthews n'ont pas été décelées dans d'autres dépressions axiales au nord de la fosse Nereus ou dans des zones interfosses. En dehors de l'axe, les anomalies magnétiques sont très amorties et le flux de chaleur est plutôt constant (environ 150 mW.m^{-2}). Un réflecteur remarquable, probablement le toit des évaporites miocènes trouvées ailleurs dans la Mer Rouge, se trouve presque partout dans cette région. Les profils de sismique réflexion révèlent une tectonique pré- ou syn-évaporitique. Les observations de l'île Zabargad, bloc soulevé de la lithosphère à 50 km à l'ouest de l'axe de la Mer Rouge, suggèrent que la croûte continentale amincie injectée de basalte est présente dans cette région en dehors des segments de fosse axiale. L'orientation de l'axe de la Mer Rouge varie d'environ 50° dans la région de transition qui est traversée par une zone de fracture (Zabargad) parallèle à la faille de la Mer Morte, et résulte probablement d'un linéament antérieur à la Mer Rouge. La tectonique complexe de cette région peut être liée à sa position vers le front d'un rift océanique se propageant vers le Nord, qui rencontre la zone de fracture Zabargad, avec formation de zones d'extension et de compression liées au soulèvement de l'île Zabargad.

Oceanol. Acta, 1984, **7**, 4, 385-398.

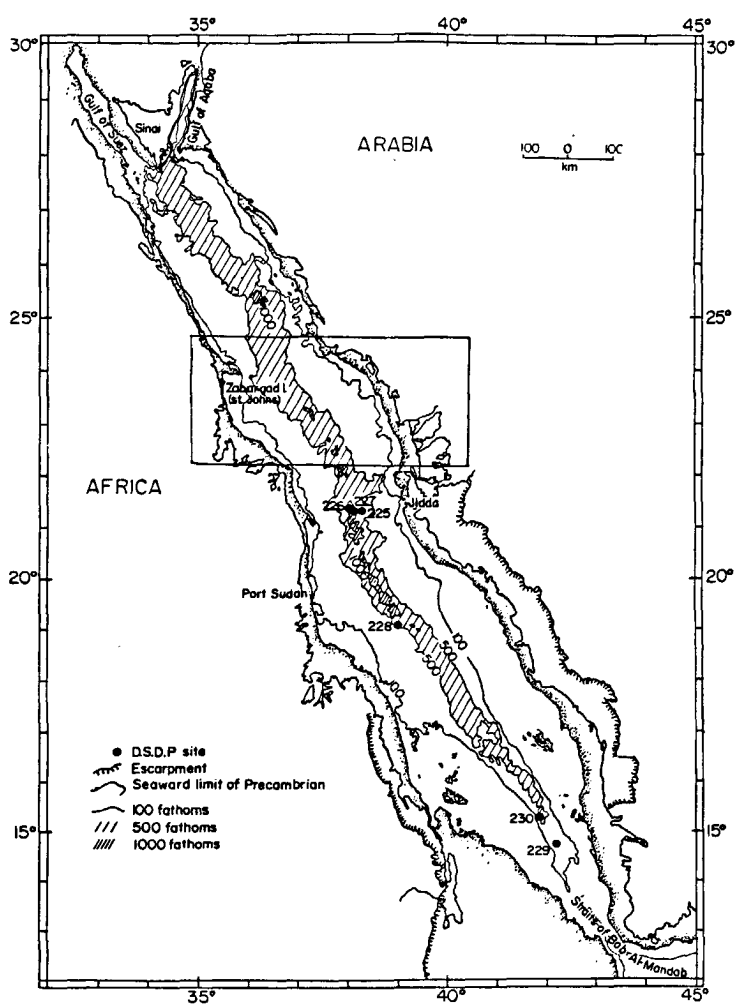

Figure 1
General morphology of the Red Sea after Coleman (1974). *Depth contours are in fathoms. Area of the present study is indicated.*

INTRODUCTION

The Red Sea-Gulf of Aden rift system is generally interpreted as an example of an embryonic and young ocean basin formed by the break up of a continent. A number of plate tectonic reconstructions have been suggested for this region (Freund, 1970; McKenzie *et al.*, 1970; Girdler, Darracot, 1972; Le Pichon, Francheteau, 1978; Richardson, Harrison, 1976).

The central Red Sea, between 22°N and 25°N, is transitional between the southern Red Sea where an axial rift valley with large magnetic anomalies is almost continuous, and the northern Red Sea where the axial valley and associated magnetic anomalies are absent (Fig. 1). The axial trough with strong magnetic anomalies of the southern Red Sea is generally interpreted as due to emplacement of oceanic crust with initiation of spreading ranging from about 1 to 5 million years ago (Vine, 1966; Allan, 1970; Phillips, 1970; Kabbani, 1970; Girdler *et al.*, 1974; Roeser, 1975). The nature of the Red Sea crust on either side of the magnetic axial trough extending close to the coastline is a subject of controversy, two main hypotheses being currently considered, namely: that it is oceanic, being emplaced by sea floor spreading-type processes (Girdler, Styles, 1974; 1976; Roeser, 1975; Hall, 1977; Styles, Hall, 1980; La Brecque, Zitellini, 1984); or that it consists of streched and thinned continental crust intruded by basaltic dykes (Drake, Girdler, 1964; Lowell, Genik, 1972; Cochran, 1983).

The Transitional Region displays discontinuous segments of an axial trough with high amplitude magnetic anomalies, separated by zones (intertrough zones) where the axial trough is absent (Searle, Ross, 1975).

Whether the crust outside the axial trough segments is oceanic, continental or something intermediary constitutes a key question in understanding the earliest stages in ocean formation by the break up of a continent. This paper reports the first results of a study based primarily on data obtained during cruises MR-79 by the vessel "Salernum" and MR-83 by the vessel "Bannock".

METHODS

Ship tracks for cruise MR-79 are shown in Figure 2. Navigation during both MR-79 and MR-83 was by satellite; sea floor depth was recorded continuously with 3.5 and 12.5 KHZ recorders. Seismic reflection profiles (Fig. 2) were obtained with a 30 KJ sparker system; magnetometric profiles (Fig. 3) with a Varian proton precession magnetometer. Heat flow was measured with a traditional thermoprobe (Gerard *et al.*, 1962; Langseth, 1965), conductivity being measured on cored bottom samples as described by Maxwell and Von Herzen (1965), and with a "pogoprobe"-type multipenetration instrument, with *in situ* determination of conductivity (Della Vedova, Pellis, 1983). Sediment samples were recovered by conventional piston and gravity coring, and hard rocks by chain-bag dredging.

MORPHOTECTONICS

The bathymetry of the area under study, as compiled by Backer *et al.* (1975) and refined by our data (Fig. 4), leads to the following observations.

Regional trend

A remarkable change by about 50° of the general Red Sea axis trend, from 310°-320° to 000°-015° occurs in the Transitional Region (Fig. 4).

Axial zone

Segments of an axial trough striking NW-SE alternate with inter-trough zones where a well developed axial

Figure 2
Ship's track during MR-79 expedition in the Red Sea transitional region. Thicker lines with lettering indicate location of seismic reflection profiles shown in Figures 6, 7, 12 and 13.

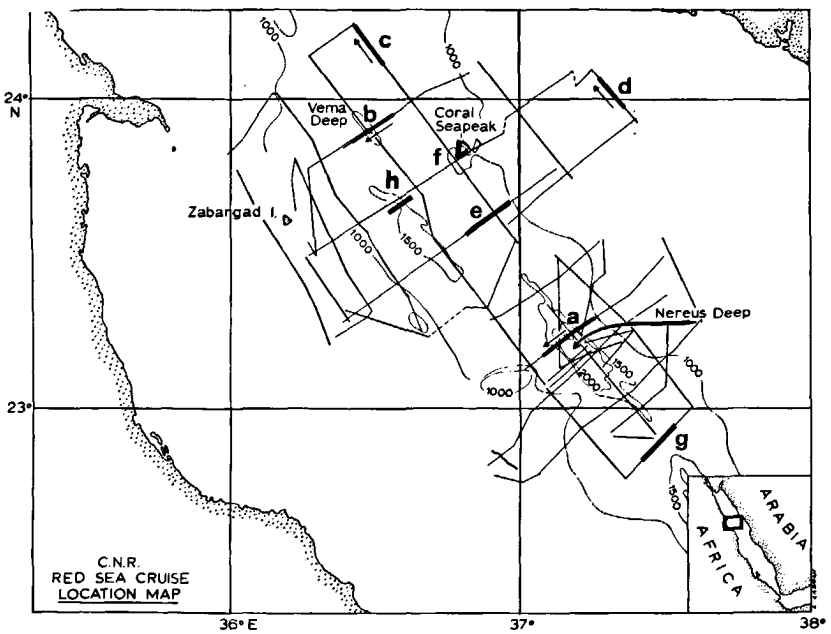

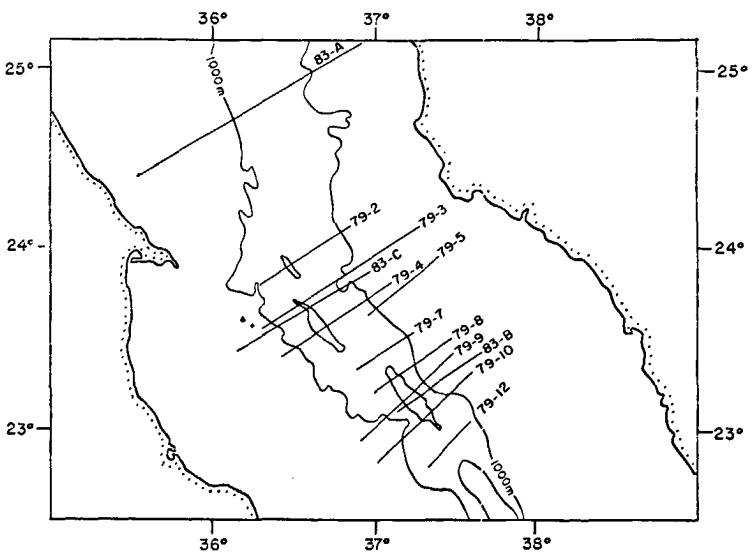

Figure 3
Location of magnetometric profiles discussed in this paper and shown in Figure 9.

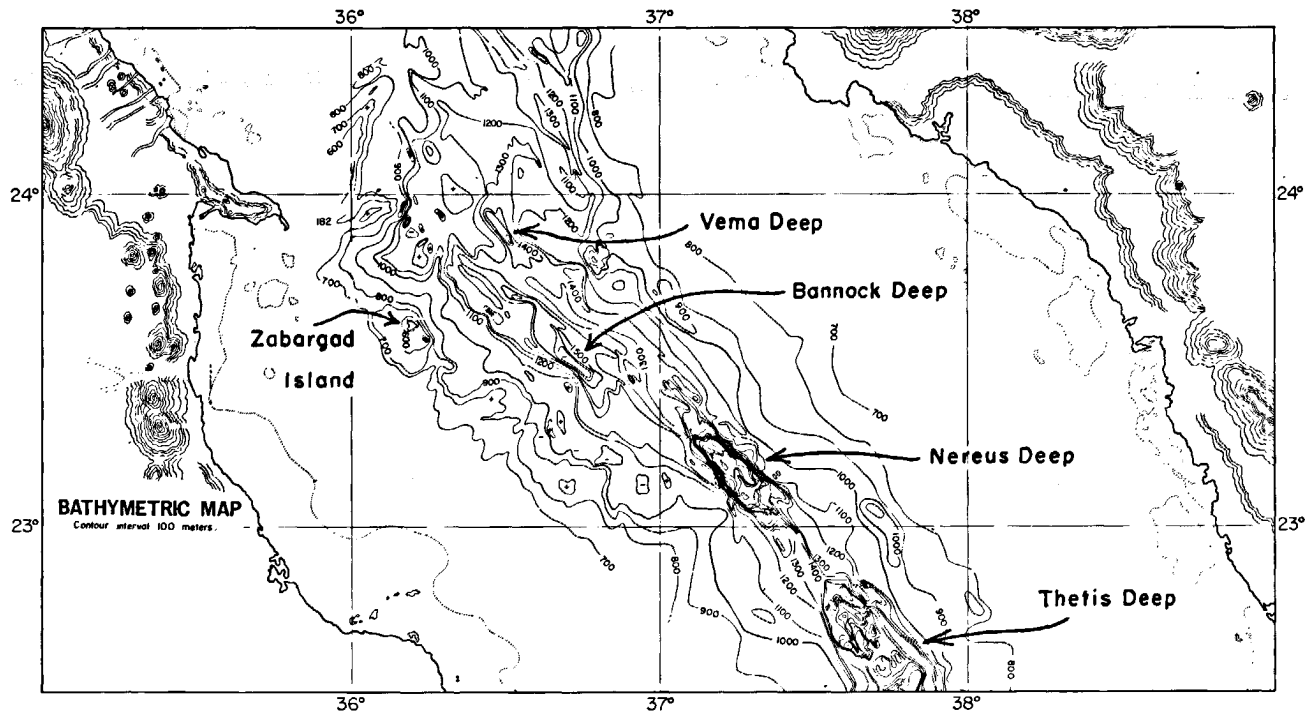

Figure 4
General morphology of the study area, from Backer et al. (1975) *and our own data.*

trough is replaced by a gentler axial depression (Fig. 3). A well developed axial trough segment, located between about 23°00′ and 23°20′N (Nereus Deep, Fig. 5), was already outlined by the data of Backer *et al.*, 1975, and further detailed by Seabeam (Pautot, 1983) and Deep-Tow (MacDonald *et al.*, in prep.) surveys. Smaller trough segments are located further north (Bannock Deep between 23°30′ and 23°40′N; Vema Deep between 23°50′ and 24°00′N); moving northward, each of these is more subdued in relief. In between, the inter-trough axial zones are characterized by a gentle gradual depression with maximum depths ranging from 1 400 to 1 500 m. The axial troughs and deeps are not aligned but are each offset laterally relative to the others (Fig. 4).

Seismic reflection profiles across the Nereus axial trough (Fig. 6*a*) indicate that the thick sediment pile, which is almost ubiquitous in this region, is interrupted at the walls of the trough. The floor of the trough is dissected by a small median ridge where the igneous basement either outcrops or is close to the sea floor. The trough is asymmetric, the NE wall being more elevated and step-like, probably due to a series of inward-facing normal faults. The axial ridge dissecting the trough is similar to the neovolcanic zone in the axial rift valley of the Mid-Atlantic Ridge in the FAMOUS area and in other axial zones of oceanic spreading centers (Fig. 7). We recovered fresh, glassy basalt from the eastern wall of the Nereus trough and from the small axial ridge (Fig. 5). A preliminary study of these basalts, including major element chemistry (Tab. 1) indicates that they are similar to basalts further south in the Red Sea, and have MORB affinity.

Seismic reflection profiles across the Bannock Deep, to the north of the Nereus trough, show continuous and

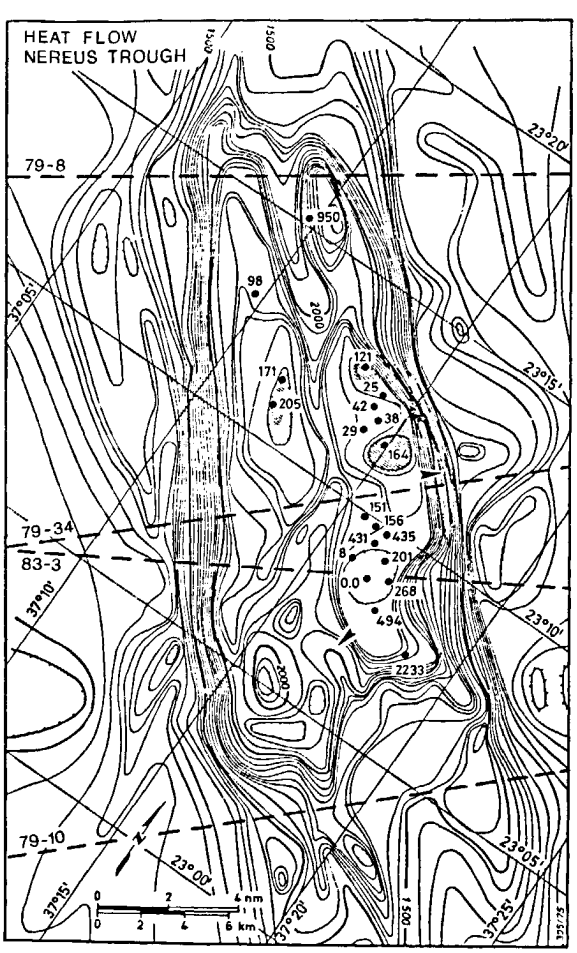

Figure 5
Morphology of the Nereus axial trough (after Backer et al., 1975), *showing heat flow values (in mW/m²), and two sites where basalt was recovered (arrows). Dashed lines indicate location of magnetometer profiles.*

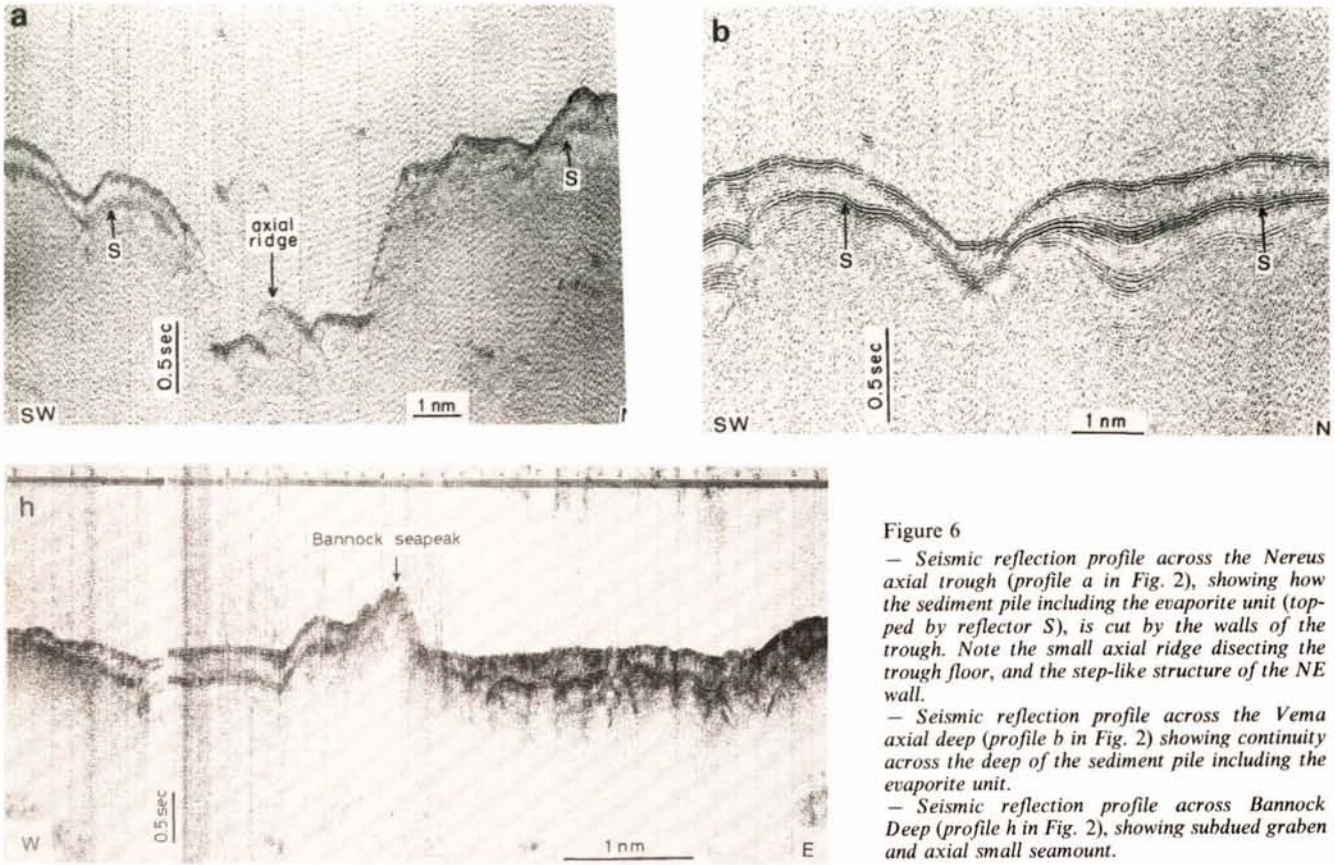

Figure 6

– Seismic reflection profile across the Nereus axial trough (profile a in Fig. 2), showing how the sediment pile including the evaporite unit (topped by reflector S), is cut by the walls of the trough. Note the small axial ridge disecting the trough floor, and the step-like structure of the NE wall.

– Seismic reflection profile across the Vema axial deep (profile b in Fig. 2) showing continuity across the deep of the sediment pile including the evaporite unit.

– Seismic reflection profile across Bannock Deep (profile h in Fig. 2), showing subdued graben and axial small seamount.

thick sediment cover across the axis, with one exception, *i.e.* profile MR 83C in Figure 6*h*, where a 500 m high relief (Bannock Seapeak) protrudes through the sediment close to the axis of a broad ($\simeq$20 km) subdued graben-like feature. This sea-mount is probably igneous, as a doleritic rock was dredged from it together with consolidated sediments. A profile a few km to the north reveals the presence of a major fault in the sediment, aligned axially with the seamount. A small seamount (Coral Seapeak of Backer *et al.*, 1975) protrudes through the sediment (Fig. 13) on the eastern margin of the Deep. Profiles across the Vema Deep further north indicate a continuous and thick sediment cover across the axis.

Axial inter-trough zones

Seismic reflection profiles across the mild depressions marking the Red Sea axis in the inter-trough zones north and south of the Nereus trough show continuous thick sediment cover across the axis, including the evaporite unit (Fig. 7). However, the sediment strata appear strongly disturbed in an axial zone roughly 10 km wide (Fig. 7). A similar continuous sediment cover was found in inter-trough zones further south between 20°N and 22°N (Searle, Ross, 1975).

Marginal areas

Outside the axial zone, the sea floor is generally smooth and thickly sedimented, with the exception of some isolated topographic highs, such as Coral Seapeak at about 23°50′N (Fig. 13). About 50 km to the west of the axial zone between 23°30′ and 23°40′N, a broad

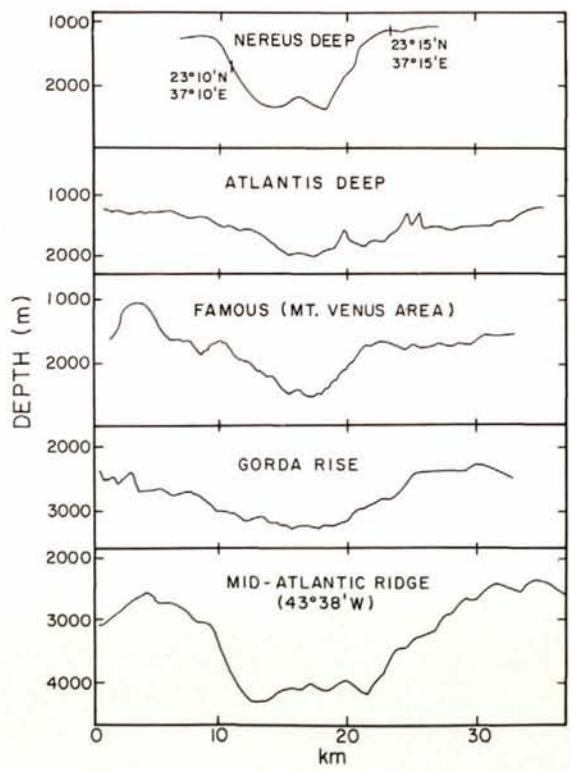

Figure 7

Morphological profile across Nereus axial trough compared with other Red Sea and oceanic axial rift zones.

Table 1

Major element chemistry of basalts from the Nereus axial trough (station MR79-34), compared with the basalts from the Southern Red Sea (from Chase, 1969) and from DSDP hole 226 (from Coleman et al., 1977).

WT. %	MR79-34A	MR79-34B	Chase 1	Chase 2	226-A	226-B	226-C	226-D
SiO_2	48.51	49.34	47.86	48.71	50.2	49.8	50.0	50.0
Al_2O_3	15.22	14.95	13.10	12.80	15.0	15.6	15.3	15.4
TiO_2	0.50	1.03	2.10	1.70	1.3	1.3	1.3	1.3
Fe_2O_3	1.34	1.41	4.82	7.80	1.5	1.5	1.5	1.0
FeO	7.30	7.30	9.16	7.46	9.2	9.1	9.2	9.7
MnO	0.14	0.21	0.26	0.25	0.15	0.14	0.12	0.12
MgO	11.34	7.39	8.30	7.30	7.9	7.8	7.9	8.2
CaO	12.40	13.19	10.60	10.20	11.6	11.5	11.5	12.0
Na_2O	1.37	2.86	2.90	2.20	2.6	2.5	2.5	2.5
K_2O	0.01	0.11	0.20	0.19	0.06	0.03	0.03	0.03
P_2O_5	0.19	0.32	0.48	0.45	0.15	0.14	0.14	0.15
Cr_2O_3	0.05	0.05	0.04	0.06	nd	nd	nd	nd
Total	98.36	100.96	100.00	100.00	100.43	100.47	100.70	101.02
CIPW Norms								
q	–	–	–	6.54	–	–	–	–
or	1.59	0.65	1.11	1.11	0.4	0.2	0.2	0.2
ab	35.36	24.20	24.63	18.34	22.1	21.3	21.3	21.1
an	20.18	27.64	21.96	24.46	29.2	31.5	30.6	30.6
ne	–	–	–	–	–	–	–	–
di	21.56	29.23	21.78	18.59	22.5	20.3	21.0	22.8
hy	6.24	2.63	4.12	14.47	13.6	15.0	15.7	11.1
ol	1.94	9.04	11.61	–	9.3	8.8	8.3	11.4
mt	0.95	2.04	6.96	11.37	nd	nd	nd	nd
il	0.41	1.96	3.95	3.19	2.5	2.5	2.5	2.5
ap	0.07	0.70	1.34	1.01	0.4	0.3	0.3	0.4

platform rises from a regional depth of about 800 m below sea level with summits above sea level forming Zabargad and Rocky Islands (Fig. 1). North of Zabargad the main trends of the Red Sea floor topography strike between 000° and 030°.

MAGNETICS

Magnetometer profiles across the Red Sea axis (Fig. 3) were processed and compared with a synthetic Vine-Matthews pattern constructed for this region, assuming a 1 cm/yr. spreading rate and projected in a direction parallel to that of the profiles (Fig. 3 and 9).

Profiles across the Nereus trough (83-B, 79-8, 79-9 and 79-10 in Fig. 5 and 9) show high amplitude axial anomalies similar to those obtained from the axial trough in the southern Red Sea, where they have been studied extensively (Vine, 1966; Allan, 1970; Phillips, 1970; Girdler *et al.*, 1974; Roeser, 1975). Profiles 79-9, 79-10 and 83-B suggest that sea floor spreading initiated here between 2 and 3 m.y.b.p. and proceeded at about 1 cm/year; on the other hand, profile MR 79-8, which crosses the trough near its northern edge (Fig. 5) shows only anomaly 1, suggesting that spreading started here not much before 1 m.y.b.p.

No high amplitude axial anomalies were detected in the inter-trough zone between the Nereus and the Thetis axial trough segments (profile 79-12, Fig. 9).

Immediately north of the Nereus trough (MR 79-7), the axial anomalies are subdued (amplitude < 50 gammas). Further north across the Bannock Deep, a narrow but strong anomaly is associated with the axial seamount (Bannock Seapeak) shown in Figure 6 (profile 83-C). Weak anomalies are found immediately to the north (profile 79-4) near an axial fault and above the Coral Seapeak. No significant anomalies were detected across

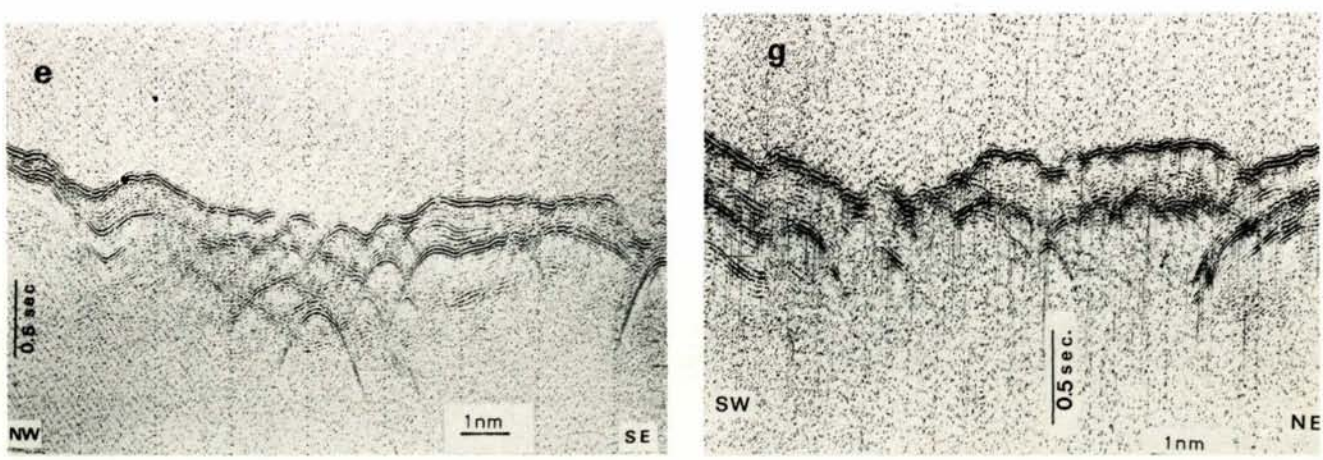

Figure 8

Seismic reflection profiles (profiles e and g in Fig. 2) of axial inter-trough zones of the transitional region.

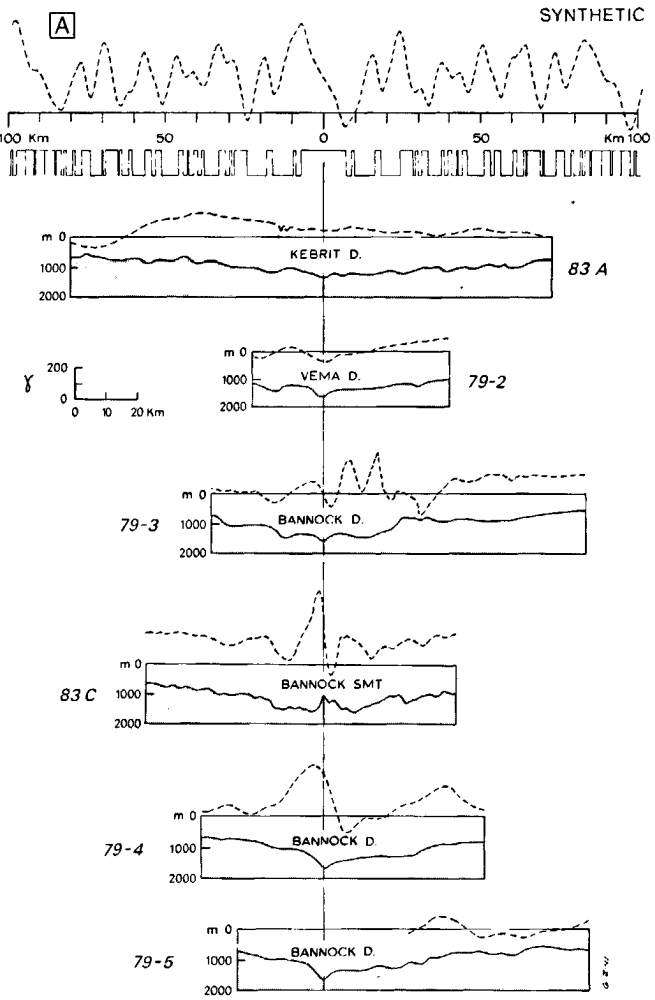

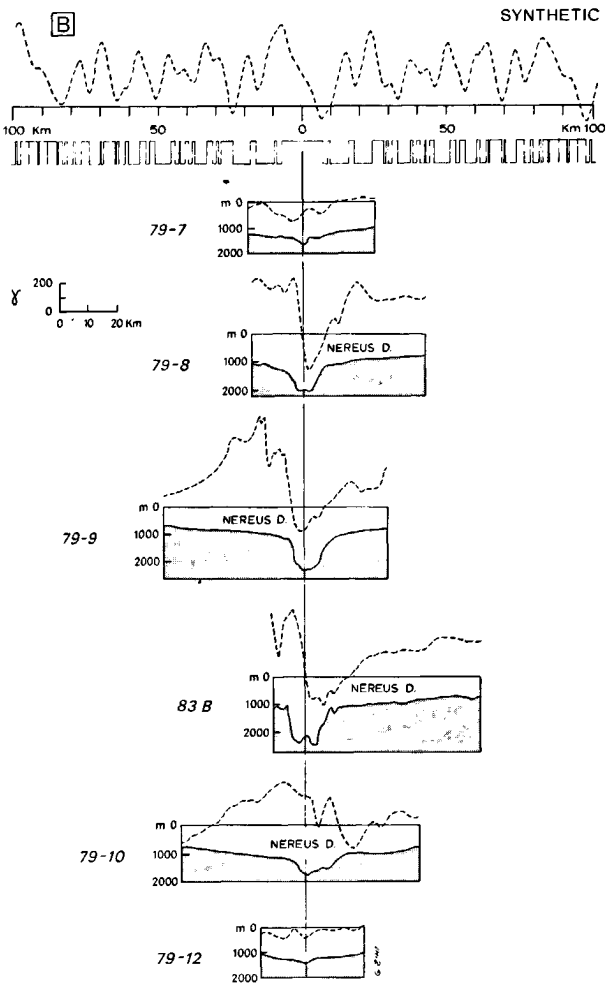

Figure 9

Magnetic anomaly and topography profiles across the axis of the Red Sea transitional region; locations of profiles are shown in Figures 3 and 5. Also shown is a synthetic magnetic anomalies profile according to the Vine-Matthews model, projected parallel to the real profiles assuming 1 cm/year spreading rate. A = profiles from the northern part of the study area. B = profiles from the southern part of the study area (Nereus trough region).

the Vema Deep (profile 79-2) and north of 24°N (profile 83-A).

These data suggest that clear-cut Vine-Matthews high amplitude axial anomalies are absent in this region of the Red Sea outside the Nereus trough, with the possible exception of anomalies associated with basaltic injections in the Bannock Deep area.

HEAT FLOW AND HYDROTHERMAL ACTIVITY

Table 2 shows temperature gradients, thermal conductivities and computed heat flows, which are plotted on Figure 10. Considering also heat flow values obtained by others (Girdler, Evans, 1977, with references therein; Backer, 1982) we can summarize as follows:

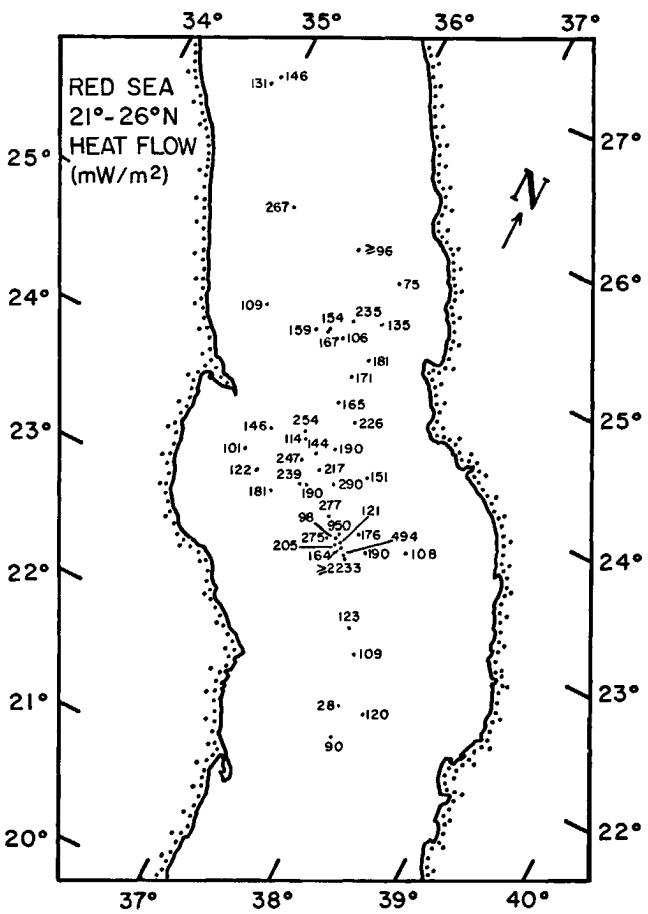

Figure 10

Heat flow values in the Red Sea transitional region (in mW/m²). In addition to values presented in this paper (Tab. 2), data from Scheuch (1973), Girdler and Evans (1977) and Backer (1983) are included.

Table 2

Thermal conductivity, bottom temperature, temperature gradient and calculated heat flow data obtained on cruises MR-79 and MR-83. MR-83 measurem were obtained with a Pogo-probe-type instrument, thermal conductivity being measured in situ.

Station number	Position			Penetration		Bottom water (°C)	Observed gradient (mK/m)	Conductivity		Calculated heat flow	
	Lat. (H) (DD MM.MN)	Long. (E) (DD MM.MM)	Depth (m)	(m)	probes N / core (m)			S=in situ N	Mean value [W/(m*K)]	(HFU)	[mW/ (m*m
MR79-01	23 04.95	36 55.97	983	3.0	— 1.10	21.72	down	5	1.04±0.04	---	---
MR79-02	23 10.92	37 05.72	1128	6.3	3 2.65	21.71	270±15	13	1.02±0.05	6.6	
MR79-03	23 21.23	37 01.07	1379	7.2	4 4.80	21.81	280±14	21	0.99±0.05	6.6	
MR79-04	23 14.24	37 28.44	937	7.0	4 3.50	21.75	178±16	18	1.07±0.06	4.5	
MR79-05	23 11.93	37 12.15	2342	down	— rock	22.02	-------	--	---	---	--
MR79-06	23 07.75	37 18.57	2216	8.0	2 4.80	21.99	⩾2977	29	0.75±0.12	⩾53.3	⩾2
MR79-07	23 11.46	37 14.70	2452	5.6	3 2.70	⩾32	205±45	14	0.80±0.14	3.9	
MR79-08	23 19.67	36 27.27	723	8.0	3 3.10	21.70	174±34	13	1.04±0.03	4.3	
MR79-09	23 29.65	36 40.13	1782	8.0	3 3.45	21.83	265±45	14	0.90±0.05	5.7	
MR79-10	23 37.19	36 55.48	1330	7.1	3 4.90	21.73	284±50	20	1.02±0.05	6.9	
MR79-11	23 46.89	37 09.84	860	8.0	3 4.00	21.70	151±23	19	1.00±0.06	3.6	
MR79-12	24 07.50	36 50.34	945	7.0	3 4.75	21.69	217±63	23	1.04±0.04	5.4	
MR79-13	23 53.77	36 29.71	1538	8.1	3 lost	21.80	254±39	--	1.00*	6.1	
MR83-01	23 04.75	37 17.54	2103	-----	- ----	22.03	------	S 3	0.88±0.04	----	--
MR83-02 I	23 42.74	36 43.86	1471	6.3	7 ----	21.85	216± 6	S 3	1.00±0.10	5.16	
II	23 42.71	36 44.00	1469	6.3	4 ----	21.85	217± 3	S 3	1.00±0.10	5.18	
MR83-03 I	26 21.32	34 53.71	1021	6.8	6 ----	21.47	178± 4	S 3	0.81±0.07	3.44	
II	26 21.21	34 53.71	1021	6.8	6 ----	21.52	167±12	S 3	0.88±0.14	3.51	
MR83-04 I	26 14.49	34 53.05	971	6.8	7 ----	21.55	167±10	S 3	0.87±0.12	3.46	
II	26 14.50	34 53.05	948	6.8	7 ----	21.53	144± 8	S 3	0.81±0.13	2.79	
MR83-05 I	24 35.81	35 39.92	603	6.8	7 ----	21.72	105± 3	S 3	1.03±0.03	2.58	
II	24 35.74	35 40.22	604	6.8	7 ----	21.72	108± 7	S 3	1.01±0.03	2.60	
MR83-06 I	24 40.46	36 08.69	984	6.0	6 ----	21.75	159±15	S 3	1.01±0.01	3.85	
II	24 40.37	36 08.94	968	6.2	6 ----	21.75	152± 6	S 3	1.03±0.02	3.75	
MR83-07	23 25.23	37 46.49	687	3.3	3 ----	21.78	100±30	S 2	1.08±0.08	2.58	
MR83-08	23 46.61	36 36.88	1363	6.4	6 ----	21.84	186± 4	S 2	1.02±0.01	4.54	
MR83-09	23 41.76	36 31.87	1493	6.3	6 ----	21.85	235±10	S 2	1.05±0.13	5.90	
MR83-10	23 46.71	36 10.44	1112	5.9	6 ----	21.78	151± 6	S 2	0.97±0.13	3.49	
MR83-11	23 28.76	36 12.90	709	6.3	5 ----	21.74	117±13	S 2	1,04±0.02	2.91	
MR83-12	23 33.77	36 01.48	807	6.6	7 ----	21.74	114± 5	S 2	0.89±0.01	2.41	
MR83-13 I	24 57.01	36 38.49	949	6.0	7 ----	21.78	141±27	S 2	1.02±0.04	3.44	
II	24 56.94	36 38.44	947	6.1	6 ----	21.79	120± 3	S 2	1.04±0.02	2.99	
MR83-14	24 49.58	36 22.78	1165	6.5	6 ----	21.76	228±11	S 2	1.03±0.02	5.61	

* estimated value.

Nereus axial trough

The temperature of the bottom water tends to be constant at 22.01° ±0.02°C. This temperature is significantly higher than the bottom temperatures outside the Nereus trough, which range from 21.47°C to 21.85°C. However, at one site within the trough (MR-79-07), where metalliferous sediments were sampled, a bottom water temperature of >32°C was measured. This hot water extends vertically for about five meters above the bottom and is probably related to a hot brine. A sharp boundary exists between the upper surface of the hot brine layer and the water above, where a temperature of 21.97°C was measured. The thermal gradient at MR 79-07 is 205°C/km giving a heat flow of 164 mW/m^2. Brine pools were detected acoustically within the Nereus trough by Backer *et al.* (1975), MacDonald *et al.* (in prep.), and by us.

At station Mt 79-06, where metalliferous sediments were also cored, no hot brines were detected, since bottom water temperatures of 21.99°C were measured. However, a very high thermal gradient of more than 3°C/m was measured in the sediment, implying a heat flow of more than 2200 mW/m^2). These data can be explained if we assume that subbottom hydrothermal circulation takes place here below the sediment, with no hydrothermal discharge through the sea floor.

Scheuch (1973) also reports two very high heat flow values (494 and 931 mW/m^2) with others ranging from 80 to 220 mW/m^2. These, together with the measurements made by Backer (1982), are shown in Figure 4.

The extreme variability of the heat flow values coupled with the presence of hot brines and metalliferous sediments, are all consistent with the occurrence beneath the axial trough of intense sub-sea-floor convective hydrothermal circulation within the basaltic crust, with the very high heat flow values suggesting the presence of a relatively shallow heat source. The discharge of hot fluids has increased bottom water temperature within the trough by about 0.5°C relative to bottom water temperature outside the trough.

Other axial deeps

A few heat flow values for the more subdued Bannock and Vema axial deeps to the north of Nereus indicate high values, close to or over 200 mW/m^2.

Off-axis areas

Our measurements in the off-axis areas, combined with the data of others, indicate that heat flow is significantly lower and more uniform (range from 80 to 180 mW/m^2) off axis than at the axis.

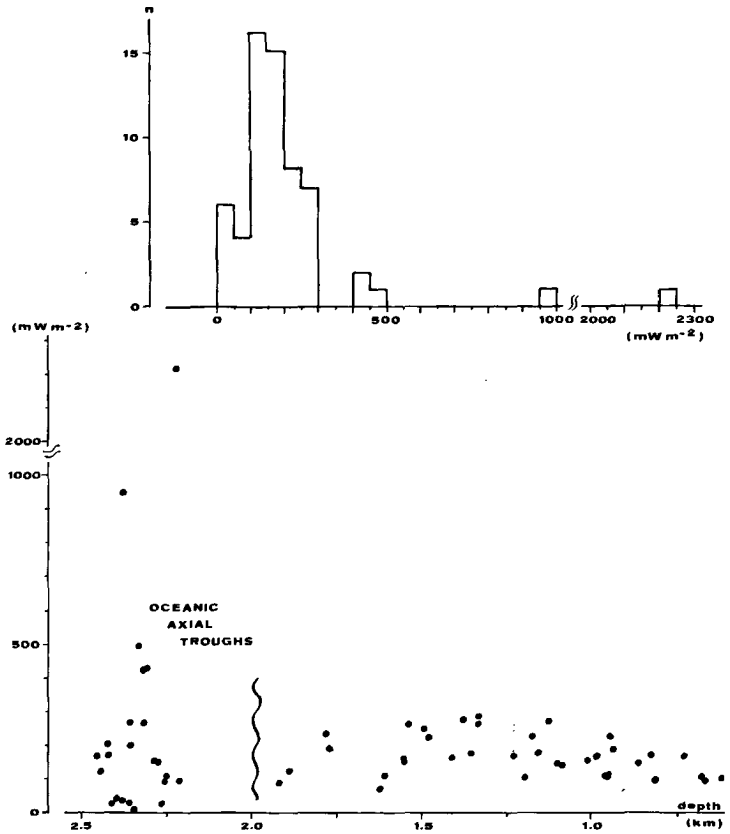

Figure 11
Top: histogram of heat flow values in the Red Sea transitional region.
Bottom: heat flow versus depth of sea floor in the Red Sea transitional region. Depth >2 km are from axial troughs.

General trends

A histogram of heat flow values for the Transitional Region is shown in Figure 11 A. The heat flow values have been plotted versus sea floor depth, where depths >2 km indicate axial troughs in Figure 11 B. Figure 12 shows the heat flow values versus estimated distance from the axis for the region from 21°40′N to 25°N, including values from eastern Egypt, taken from Morgan *et al.*, 1980, and plotted against distance from the Red Sea shore.

SEDIMENTARY STRUCTURES AND STRATIGRAPHY

A prominent seismic reflector beneath a sediment layer with thickness corresponding to 0.2 to 0.7 seconds (two way travel time) is ubiquitous except beneath the Nereus axial trough, and in the vicinity of igneous structures in the Bannock Deep area, *i.e.*, the Coral and Bannock Seapeaks. The reflector is probably reflector S found in most of the Red Sea (Knott *et al.*, 1966; Ross *et al.*, 1969; Phillips, Ross, 1970; Ross, Schlee,

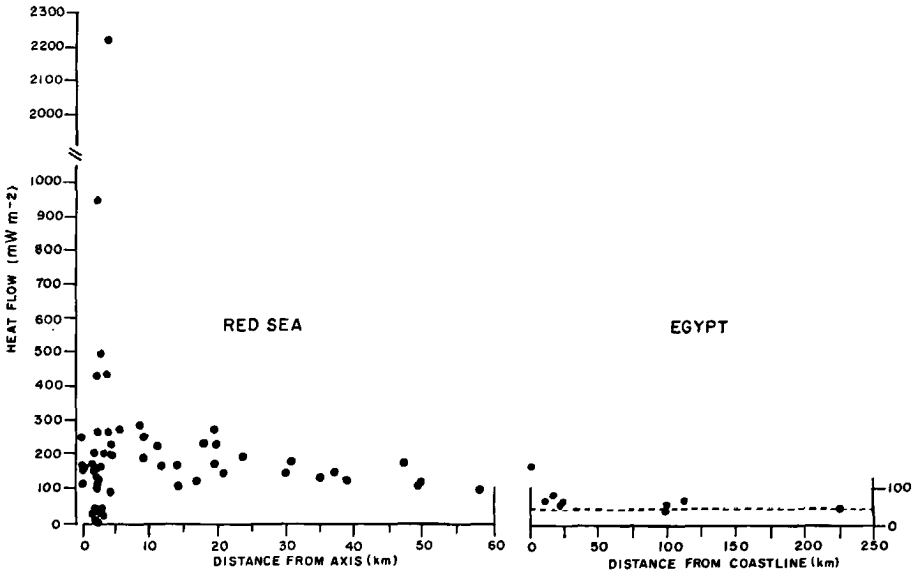

Figure 12
Plot of heat flow versus distance from axis in Red Sea transitional region, and of heat flow versus distance from Red Sea shore in eastern Egypt. Heat flow data for Egypt are from Morgan et al. (1980).

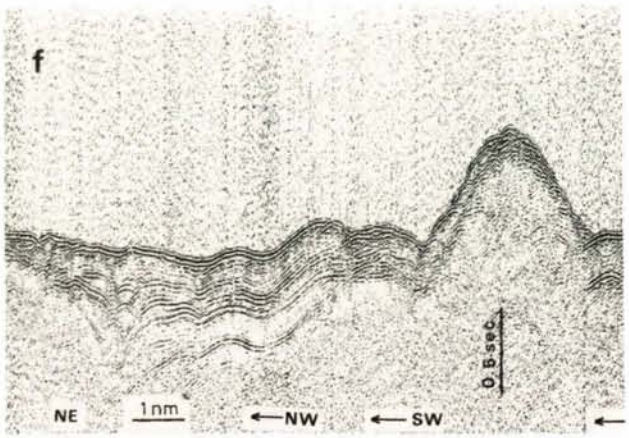

Figure 13
Seismic reflection profile (profile f in Fig. 2) from the vicinity of a small seamount (Coral Sea Peak).

layers and fragments, and by dark sapropelitic levels at the Pleistocene-Holocene boundary. Previous studies of the lithified layers (Milliman, 1971, 1977; Milliman *et al.*, 1969) also supported by oxygen isotopic analyses (Tab. 3), suggest that they originated by deposition from mesohaline Red Sea waters, during a glacial maximum. Sapropels have been recorded previously in the Red Sea, ranging in age from lower Pliocene to upper Pleistocene (Muller, 1976; Stoffers, Kuhn, 1974; Besse, Taviani, 1982).

DISCUSSION

Initial emplacement of oceanic crust

In this region, emplacement of oceanic crust within a narrow axial zone, with formation of Vine-Matthews

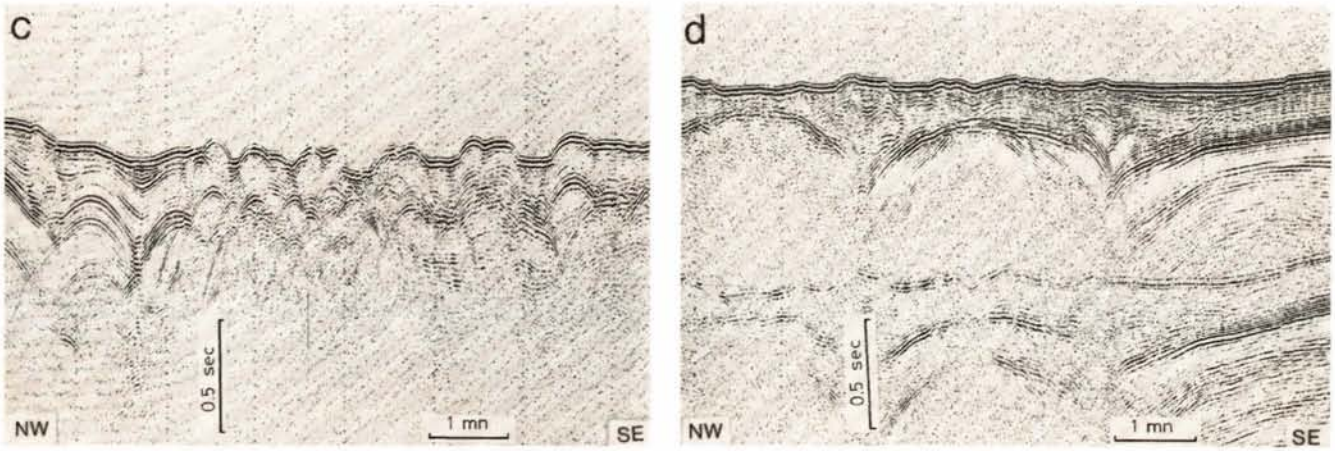

Figure 14
Seismic reflection profiles (profiles c and d) in thickly sedimented areas to the side of the axial zone. Location of profiles is in Figure 2.

1973) and generally interpreted as a major unconformity separating the top of an evaporitic sequence of Miocene age from the Plio-Pleistocene sediments. This interpretation is supported by sampling (DSDP Leg 23 and commercial wells) with recovery of anhydrite and halite (Whitmarsh *et al.*, 1974; Ross *et al.*, 1972; Stoffers, Kuhn, 1974).

Unconformities and sediment disturbances are observed below reflector S, suggesting a complicated intra-evaporitic history with intense pene-contemporaneous tectonic activity and post-depositional salt movements, as illustrated by the diapir-like structures in Figure 14.

Above the evaporites, the sequence is monotonous and relatively undisturbed, being about 100-200 m thick and consisting mainly of marly calcareous oozes and claystones (Stoffers, Ross, 1974). Cores from the uppermost part of the sequence consist of calcareous nanno oozes of late Pleistocene-Holocene age, with carbonates (low Mg-calcite, high Mg-calcite and aragonite) as main components, followed by detrital minerals such as quartz, feldspars, micas and clay minerals; sulfides and anhydrite are seldom present. The lithologic monotony of the sediment cores is interrupted by lithified

magnetic stripes as in the classical sea floor spreading model (which we call here "true" sea floor spreading), is clearly found only within the Nereus trough, as supported by its morphotectonic and thermal structure and the nature of the basalts outcropping on its floor. A northward progressive opening of the Nereus oceanic segment is suggested by the magnetic anomalies; sea floor spreading appears to have started at Nereus between 2 and 3 m.y.b.p. except close to the northern tip of the trough where it started more recently. Axial inter-trough zones immediately to the south and north of the Nereus trough are free of high amplitude magnetic anomalies, leading to the inference that true" sea floor spreading has not begun in these zones. Thus, the Nereus trough can be considered a mini-propagating oceanic segment of limited ($\pm$40 km) length. The Bannock and Vema Deeps to the north are sediment-filled subdued grabens morphologically different from steep axial rift valleys. However, the isolated igneous body protruding through the sediment at the axis of the Bannock Deep, and the axial fault detected immediately to the north of this igneous body, may indicate an initial injection of basaltic (oceanic) crust along an axial

Table 3

δO^{18} and δC^{13} values of lithified carbonate layers dredged from the Central Red Sea. Carbonates were reacted with 100% phosphoric acid at 49.5°C and then analyzed using a Nuclide 6" Mass Spectrometer of Lamont-Doherty Geological Observatory. Results are reported in δ-notation defined as per mil difference relative to PDB standard according to the equation $\delta = \left(\frac{R_{sample}}{R_{standard}} - 1\right) 1\,000$ *where* $R = {}^{18}O/{}^{16}O$ *or* $R = {}^{13}C/{}^{12}C$.

Station	Beginning	End	Water depth (m)	Mineralogy	δO^{18} PDB	δC^{13} PDB
MR79-34	23°10.89'N 37°16.25'E	23°11.89'N 37°17.84'E	1 749/1 172	Aragonite, Calcite	+ 6.63	+ 3.73
MR79-41	23°49.32'N 36°49.58'E	23°49.70'N 36°49.69'E	722/578	Calcite, Aragonite	+ 4.02	+ 2.82
MR83-45	23°33.92'N 36°01.89'E	23°34.68'N 36°03,03'E	699/650	Calcite, Aragonite	+ 3.26	+ 2.13

fissure, suggesting the very first stage of "true" sea floor spreading. The absence of igneous bodies and of axial high amplitude magnetic anomalies suggests that the Vema Deep is further away from developing into a spreading segment. Absence of morphotectonic and magnetic features typical of spreading centers indicates that the axial regions north of the Vema Deep do not yet approach a "true" sea floor spreading regime.

A possible interpretation is that initiation of "true" sea floor spreading follows a temporal progression from south to north in the Red Sea Transitional Region, in agreement with a rift propagation model proposed for the southern Red Sea (Courtillot, 1980; 1982). Our data from the Red Sea Transitional Region suggest that: a) sea floor spreading initiates at discrete spots along the axis; b) a time-space progression exists in the activation of each spot, *i.e.*, Nereus spot about 2-3 m.y. old; Bannock spot: just being activated; Vema spot: not yet activated; north of Vema: inactive; c) rift propagation proceeds axially from each spot, which develops into a "mini-propagating rift" as exemplified by the Nereus segment; d) the spots are not necessarily aligned axially, being offset in an "en echelon" pattern.

Nature of the crust in the transitional region

The crust underlying the Red Sea transitional region outside the Nereus oceanic segment does not appear to have been produced by "true" sea floor spreading. This statement is in line with: a) absence of clear Vine-Matthews magnetic stripes; b) heat-flow data which outside the axis is relatively constant (Fig. 12) rather than following an exponential decrease with distance from the axis as observed generally in young oceanic crust; c) seismic velocities lower than those typical for oceanic crust found in several areas of the Red Sea outside the axis (Drake *et al.*, 1959; Drake, Girdler, 1964). Observations on Zabargad island can help in understanding the nature of the crust in this region. The island is an uplifted fragment of Red Sea crust and upper mantle consisting of mantle-derived peridotites in tectonic contact with a metamorphic unit and with a sedimentary sequence ranging in age from Cretaceous-Paleocene to Pleistocene (Bonatti *et al.*, 1981; 1983). The Zabargad metamorphic unit is probably equivalent to the Paleozoic Panafrican unit outcropping in eastern Egypt and Sudan (Dixon, 1979).

This metamorphic unit is criss-crossed at Zabargad by basaltic-doleritic dykes, which on the western part of the island account for as much as 20-30 per cent of the unit. It is tempting to extrapolate and suggest that continental metamorphic rocks injected by basaltic dykes are present also in the crust of the Red Sea Transitional Region outside the axial troughs.

The subdued magnetic anomalies outside the Nereus trough are consistent with the presence of stretched continental crust injected with basaltic dykes as modeled by Frazier (1970) and Cochran (1982), though they also have been modeled assuming an oceanic-type crust produced by diffuse basaltic injections (La Brecque, Zitellini, in press).

We conclude that the crust in the transitional region outside the magnetic axial troughs consists probably of attenuated, stretched continental rocks criss-crossed by basaltic injections. Cochran (1983) has reviewed all available evidence and has concluded that the presence of stretched, attenuated, down-faulted continental crust, as in McKenzie's (1978) model, best fits the evidence. Assuming a pre-sea floor spreading phase of diffuse extension and dyke injection (Cochran, 1983), where the frequency of injections increases towards the axis, the observed 20-30% basaltic dykes within the metamorphic unit exposed on Zabargad, located about 50 km from the axis, suggests that a large fraction of the crust in the transitional region might be basaltic, increasing towards the axis. Generation by "true" sea floor spreading is not implied by the presence of quasi-basaltic crust of this type.

This view can be reconciled with the amount of separation between Africa and Arabia required by plate reconstructions. Diffuse extension by faulting of the continental crust and by dyke injection, if lasting over a long enough period, can account for over 100 km widening of the basin (Cochran, 1983). Our seismic reflection profiles suggest that the Transitional Region was tectonically very active before reflector S time, *i.e.*, late Miocene.

Zabargad fracture zone

Satellite radar imagery suggests that a major tectonic lineation intersects the Red Sea transitional region roughly at the latitude of Zabargad island (Crane, Bonatti, 1984) with strike about 015°, that is, parallel to the

gulf of Aqaba-Dead Sea fault. We name this feature the Zabargad Fracture Zone (Fig. 4,15). Roughly at this latitude, the regional direction of the Red Sea axis changes, forming a knee with an angle of about 50° (Fig. 4), from NNW-SSE to N-S (Fig. 4) close to the direction of the proposed fracture zone. Seismic reflection profiles show that a 20° structural trend is important in this area (Fig. 16). Moreover, one of the structural alignments observed on Zabargad strikes 000°-020° (Bonatti *et al.*, 1983). An alignment of igneous alkaline complexes on the African side (Garson, Krs, 1976; Serencsits *et al.*, 1981) is along the same direction. These igneous complexes have been dated as ranging from Paleozoic to Jurassic (Serencsits *et al.*, 1981), implying that the lineament has been intermittently active. The Zabargad Fracture Zone might result from post-Mesozoic reactivation of this ancient paleoshear zone.

Impingement of the propagating oceanic rift with the fracture zone

Courtillot (1982) has suggested that rift propagation takes place between "locked zones", that is, zones which are more resistant to rifting and are intensely deformed before they are penetrated by a propagating rift. The Red Sea transitional region and the Zabargad fracture zone with its parent paleoshear can be considered a "locked zone". Impingement of the propagating axial rift against the Zabargad fracture/Paleoshear zone may explain in part the complex geology of the transitional region. Compressional regimes may develop in areas near the front of a propagating rift (Hey *et al.*, 1980; Bonatti, Crane, 1982; Courtillot, 1982). Crane and Bonatti (1984) suggest that since the axial rift impinged against the paleoshear zone at an oblique angle (Fig. 15), the eastern portion of the transitional region might have been subjected preferentially to extension, the western to compression. This compression, and compressional stresses related to fracture zone tectonics (Bonatti, 1978), may be responsible for the uplift of the Zabargad lithospheric sliver through an attenuated and stretched continental crust at some time during the Cenozoic. The Zabargad mantle protrusion may be the equivalent of mantle protrusions found in older margins. One example, reported by Boillet *et al.* (1980), is that of serpentine diapirs found near the boundary between thinned continental crust and oceanic crust at the Iberian margin of the Atlantic.

The oceanic axial rift abuts in the southern Red Sea against the Hanish-Bidu-Dubbi lineament, to the south of which the rift is displaced in Afar. According to Courtillot (1982), Afar constitutes a deformed "locked zone" between the southern tip of the Red Sea rift and the western end of the Gulf of Aden rift. The Red Sea Transitional Region, with its pattern of "en echelon" axial rift segments, some already with oceanic crust but where "true" sea floor spreading has barely started, is reminiscent of Afar with its "en echelon" pattern of axial basaltic ranges (Barberi, Varet, 1977). Both regions may develop continuous axial zones of spreading in the future, as seen presently in the Gulf of Aden and in portions of the southern Red Sea.

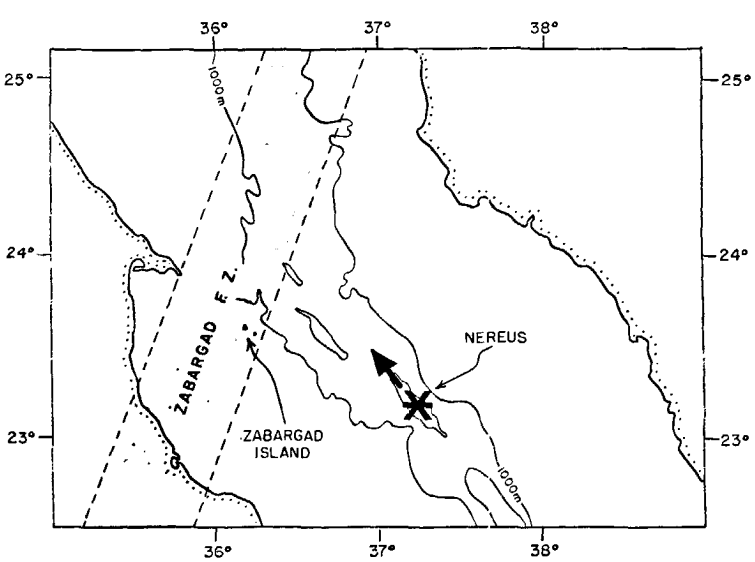

Figure 15

Schematic model illustrating location of the Zabargad Fracture Zone (from Crane, Bonatti, 1984) and of Nereus oceanic segment, which acts as a northwards propagating rift.

Acknowledgements

The field work was sponsored by the Italian CNR (Consiglio Nazionale delle Richerche). We are grateful to the captain, officers and crew of the vessels Salernum and Bannock as well as to our colleagues in both cruises for their collaboration.

We are also grateful to J. Cochran, J. La Brecque, T. Aitken and N. Zitellini for their help in elaborating the magnetometric data and for many constructive comments on this work; and to D. Breger for assistance throughout the project. Research sponsored by C.N.R., by O.N.R. Contract N00014-80-C-0098/T and by N.S.F. grant OCE 83-15933. Contribution No. 3682 from Lamont-Doherty Geological Observatory of Columbia university, and No. 000 from the Istituto di Geologia Marina del CNR.

REFERENCES

Allan T.D., 1970. Magnetic and gravity fields over the Red Sea, *Philos. Trans. R. Soc. London*, **A267**, 153-180.

Backer H., Lange K., Richter H., 1975. Morphology of the Red Sea central Graben between Subair Islands and Abul Kizaan, *Geol. Jahrb.*, **D13**, 79-123.

Barberi F., Varet Y., 1977. Volcanism of Afar: small-scale plate tectonics implications, *Geol. Soc. Am. Bull.*, **88**, 1251-1266.

Becker K., 1981. Heat flow studies of spreading centers hydrothermal processes, *Ph. D. Thesis, Univ. California, San Diego*, 149 p.

Besse D., Taviani M., 1982. The last Quaternary sapropelitic level in the Red Sea: its micropaleontological–mineralogical characteristics and paleoceanographical significance, *INQUA XI Congress, Moscow* 1982, *abstracts* 1, 36.

Boillot G., Grimaud S., Mauffret A., Mougenot D., Kornprobst J., Mergoil G., Torrent G., 1980. Ocean-continent boundary off the Iberian margin: a serpentine diapir west of the Galicia Bank, *Earth Planetary Sci. Lett.*, **48**, 23-34.

Bonatti E., 1978. Vertical tectonism in oceanic fracture zones, *Earth Planetary Sci. Lett.*, **37**, 369-379.

Figure 16

Main structural trends in the region close to Zabargad Island, based on topographic and seismic reflection profiles. Dotted lines indicate location of seismic reflection profiles. Note how a trend parallel to the Zabargad Fracture Zone (≃20°) meets a trend parallel to the Red Sea axis.

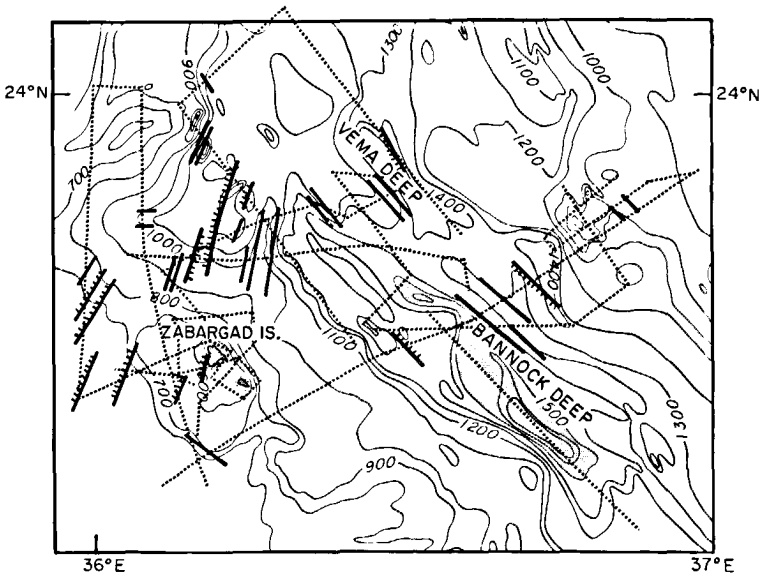

Bonatti E., Crane K., 1982. Oscillatory spreading explanation of anomalously old uplifted crust near oceanic transforms, *Nature*, **300,** 343-445.

Bonatti E., Hamlyn P. R., Ottonello G., 1981. The upper mantle beneath a young oceanic rift: peridotites from the island of Zabargad, *Geology*, **9,** 474-479.

Bonatti E., Clocchiatti R., Colantoni P., Gelmini R., Marinelli G., Ottonello G., Santacroce R., Taviani M., Abdel-Meguid A. A., Assaf H. S., El Tahir M. A., 1983. Zabargad (St. John) Island: an uplifted fragment of Red Sea lithosphere, *J. Geol. Soc. London*, **140,** 677-690.

Cochran J. R., 1983. A model for the develoment of the Red Sea, *Am. Assoc. Petrol. Geol. Bull.*, **67,** 41-69.

Coleman R. G., 1974. Geological background of the Red Sea, *Initial Rep. DSDP*, **23,** 813-820.

Coleman R. G., Fleck R. J., Hedge C. E., Ghent E. D., 1977. The volcanic rocks of southwest Saudi Arabia and the opening of the Red Sea, *Mineral Resources Bull. 22D, Red Sea Research, Jaddah, Saudi Arabia*, D1-D30.

Courtillot V. E., 1980. Opening of the Gulf of Aden and Afar by progressive tearing. *Phys. Earth Planetary Inter.*, **21,** 343-350.

Courtillot V. E., 1982. Propagating rifts and continental breakup, *Tectonics*, **1,** 239-250.

Crane K., Bonatti E., 1984. Structural analysis of the Red Sea margins using the space shuttle imaging radar (SIR-A): implications for a propagating rift, submitted to *Tectonics*.

Della Vedova B., Pellis G., 1984. Misure di flusso di calore nei mari italiani, *Rapporto Progetto Finalizzato Oceanografia*, CNR Roma, Italy, in press.

Dixon T. H., 1979. The evolution of the continental crust in the Late Precambrian Egyptian shield, *Ph. D. Thesis, Univ. California, San Diego*, 231 p.

Drake C. L., Girdler R. W., 1964. A geophysical study of the Red Sea, Geophys., *J. R. Astron. Soc.*, **8,** 473-495.

Drake C. L., Girdler R. W., Landisman M., 1959. Geophysical measurements in the Red Sea, in: Preprints of Abstracts to be presented at Afternoon Sessions, Inter. Oceanogr. Congress, edited by M. Sears, *Am. Assoc. Adv. Sci., Washington D.C.*, **20.**

Frazier S. B., 1970. Adjacent structures of Ethiopia: that portion of the Red Sea coast including Dahlak, Kebir Island and the Gulf of Zula, *Philos. Trans. R oc. London*, **A267,** 131-141.

Freund R., 1970. Plate tectonics of the Red Sea and East Africa, *Nature*, **228,** 453.

Garson M. S., Krs M., 1976. Geophysical and geological evidence of the relationship of the Red Sea transverse tectonic to ancient fractures, *Geol. Soc. Am. Bull.*, **87,** 169-181.

Gerard R., Langseth M. G., Ewing M., 1962. Thermal gradient measurements in the water and bottom sediment of the western Atlantic, *J. Geophys. Res.*, **67,** 2, 785-803.

Girdler R. W., Darracott B. W., 1972. African poles of rotation, Comments Earth Science, *Geophysics*, **2,** 131-138.

Girdler R. W., Styles P., 1974. Two stage Red Sea floor spreading, *Nature*, **247,** 1-11.

Girdler R. W., Styles P., 1976. The relevance of magnetic anomalies over the southern Red Sea and Gulf of Aden to Afar, in: *Afar between continental and oceanic rifting*, edited by A. Pilger and A. Rosler, Schweizebart, Stuttgart, 156-170.

Girdler R. W., Evans T. R., 1977. Red Sea heat flow, *Geophys. J. R. Astron. Soc.*, **51,** 245-251.

Hall S. A., 1977. A total intensity magnetic anomaly map of the Red Sea and its interpretation. *Ph. D. thesis, Univ. New Castle upon Tyne*, 260 p.

Hey R., Duennebies F. K., Morgan W. J., 1980. Propagating rifts on mid-ocean ridges, *J. Geophys. Res.*, **85,** B7, 3647-3658.

Rimmerblau D. M., 1970. *Process analysis by statistical methods John Wiley and Sons, Inc.*, 463, *New York*.

Kabbani F. K., 1970. Geophysical and structural aspects of the central Red Sea rift valley, *Philos. Trans. R. Soc. London*, **A267,** 89-97.

Knott S. T., Bunce E. T., Chase R. L., 1966. Red Sea seismic reflection studies, in: The world rift system, Geol. Surv., Can. Spec. Pap., 66-14, 78-97.

La Brecque J. L., Zitellini N., 1983. Continuous seafloor spreading in the Red Sea: an alternative interpretation of the magnetic anomaly pattern, *Am. Assoc. petrol. Geol.*, in press.

Langseth M. C., 1965. Techniques of measuring heat flow through the ocean floor, in: Terrestrial heat flow, *Geophys. Monogr.*, **8,** 59-77, Washington.

Le Pichon X., Francheteau J., 1978. A plate tectonics analysis of the Red Sea-Gulf of Aden Area, *Tectonophysics*, **46,** 369-406.

Lowell J. D., Genik G. J., 1972. Sea-floor spreading and structural evolution of the southern Red Sea, *Am. Assoc. Petrol. Geol. Bull.*, **56,** 247-259.

Maxwell A. E., Von Herzen R., 1959. The measurement of thermal conductivity of deep sea sediments by a needle probe method, *J. Geophys. Res.*, **64,** 10, 1557-1563.

McKenzie D. P., 1978. Some remarks on the development of sedimentary basins, *Earth Planetary Sci. Lett.*, **40,** 25-32.

McKenzie D. P., Davies D., Molnar P., 1970. Plate tectonics of the Red Sea and East Africa, *Nature*, **226,** 243-248.

Milliman J. D., 1971. Carbonate lithification in the deep sea, in: *Carbonate cements*, edited by O. P. Bricker, Johns Hopkins Univ., Studies in Geology, **19,** 95-102.

Milliman J. D., 1977. Interstitial waters of late Quaternary Red Sea sediments and their bearing on submarine lithification, in: Red Sea Research 1970-1975, *Miner. Resour. Bull.*, **22,** M1-M6.

Milliman J. D., Ross D. A., Ku T. L., 1969. Precipitation and lithification of deep-sea carbonate in Red Sea, *J. Sediment. Petrol.*, **39,** 724-736.

Morgan P., Swanberg C. A., Boulos F. K., Hennin S. F., El Sayed A. A., Basta N. Z., 1980. Geothermal studies in Northeast Africa, *Annal. Geol. Surv. Egypt.*, **10,** 971-987.

Muller C., 1976. Nannoplankton—Gemeinschaftern aus dem jung—is Quarter des Golfs von Aden und dem Roten Meeres, *Geol. Jahrb.*, **D17,** 33-37.

Pautot M. G., 1983. Les fosses de la Mer Rouge : approche géomorphologique d'un stade initial d'ouverture océanique réalisée à l'aide du Seabeam, *Oceanol. Acta*, **6**, 3, 235-244.

Phillips J. D., 1970. Magnetic anomalies in the Red Sea, *Philos. Trans. R. Soc. London*, **A 267**, 205-217.

Phillips J. D., Ross D. A., 1970. Continuous seismic reflection profiles in the Red Sea, *Philos. Trans. R. Soc. London*, **A 267**, 143-152.

Richardson E. S., Harrison C. G. A., 1976. Opening of the Red Sea with two poles of rotation, *Earth Planetary Sci. Lett.*, **30**, 135-142.

Roeser H. A., 1975. Detailed magnetic survey of the southern Red Sea, *Geol. Jahrb.*, **13**, 131-153.

Ross D. A., Schlee J., 1973. Shallow structure and geologic development of the southern Red Sea, *Geol. Soc. Am. Bull.*, **84**, 3827-3848.

Ross D. A., Hays E. E., Allstrom F. C., 1969. Bathymetry and continuous seismic profiles of the hot brine region of the Red Sea, in: *Hot brines and recent heavy metal deposits in the Red Sea*, edited by E. T. Degens and D. A. Ross, New York, Springer-Verlag, 82-97.

Ross D. A. *et al.*, 1972. Deep Sea Drilling Project in the Red Sea, *Geotimes*, **17**, 24-26.

Scheuch J., 1973. Waermestrom dichtemessungen im Roten Meer zwischen 19° und 26° nordlicher Breite (Gebiet der Laugentiefs), *Zietschr. Geophys.*, **39**, 859-862.

Searle R. C., Ross D. A., 1975. A geophysical study of the Red Sea axial trough between 20.5° and 22°N, *Geophys. J. R. Soc. London*, **43**, 555-572.

Serencsits C. McC., Faul H., Foland K. A., Hussein A. A., Lutz T. M., 1981. Alkaline. Ring complexes in Egypt: their ages and relationship in time, *J. Geophys. Res.*, **86**, B4, 30009-3013.

Shipboard Scientific Staff, CNR, Red Sea Cruise, 1979. *Geology of the Red Sea between 23° and 25°N, Preliminary results, geodynamic evolution of the Afro-Arabian rift system*, Acc. Naz. Lincei, Rome, 607-613.

Stoffers P., Kuhn R., 1974. Red Sea evaporites: a petrographic and geochemical study, edited by R. B. Whitmarsh, O. E. Weser, D. A. Ross *et al.*, *Initial Rep. DSDP*, **23**, 821-847.

Stoffers P., Ross D. A., 1974. Sedimentary history of the Red Sea, edited by R. B. Whitmarch, O. E. Weser, D. A. Ross *et al.*, *Initial Rep. DSDP*, **23**, 849-865.

Styles P., Hall S. A., 1980. A comparison of the seafloor spreading histories of the western Gulf of Aden and the central Red Sea, in: *Geodynamic evolution of the Afro-Arabian rift system*, Accad. Naz. Lincei, Rome, 587-606.

Vine F. J., 1966. Spreading of the ocean floor—new evidence, *Science*, **154**, 1405-1415.

Vine F. J., Matthews D. H., 1963. Magnetic anomalies over oceanic ridges, *Nature*, **199**, 947.

Whitmarsh R. B., Weser O. E., Ross D. A. *et al.*, 1974. *Initial Reports of the Deep Sea Drilling Project*, **23**, Washington, D.C., US Government Printing Office.